International Journal of Information, Control and Computer Sciences
ISSN: 2517-9942
Vol:10, No:4, 2016

Image Enhancement Algorithm of Photoacoustic Tomography Using Active Contour Filtering

Prasannakumar Palaniappan, Dong Ho Shin, Chul Gyu Song

***Abstract*—**The photoacoustic images are obtained from a custom developed linear array photoacoustic tomography system. The biological specimens are imitated by conducting phantom tests in order to retrieve a fully functional photoacoustic image. The acquired image undergoes the active region based contour filtering to remove the noise and accurately segment the object area for further processing. The universal back projection method is used as the image reconstruction algorithm. The active contour filtering is analyzed by evaluating the signal to noise ratio and comparing it with the other filtering methods.

***Keywords*—**Contour filtering, linear array, photoacoustic tomography, universal back projection.

I. Introduction

AN emerging imaging modality photoacoustic tomography (PAT) is non-invasive and nonionizing and has high sensitivity, average imaging depth, good spatial and temporal resolution. A short laser pulse is induced into the highly scattering biological specimen known as photoacoustics (PA) or laser induced ultrasonography. A theromoelastic effect is formed when the laser heats up the absorbing part of the biological tissues to a fraction of degree which results in the excitation of ultrasonic waves [1], [2]. These ultrasonic signals are collected using an ultrasonic transducer. While detecting these ultrasonic pressure signals, the photoacoustic images of specimens are formed [3]. Blood vessels up to a depth of few centimeters can be imaged when absorption spectrum of a specimen is found by excitation of multiple wavelength. Other optical imaging modalities, such as optical coherence tomography, have a high resolution imaging; but, it has the limitation of scanning depth only to few millimeters due to the nature of optical scattering [4]. PAT overcomes this limitation and can image up to a depth of few centimeters [5]-[7].

A high frequency real-time PA microscopy system that can image the microvasculature of living subjects up to a depth of few mm [13] was reported recently. The PAT has prospects in various aspects such as melanoma detection, PA endoscopy, PA tomography of genes expression, Doppler PA tomography, PA mapping of sentinel lymph nodes and PA along with thermoacoustic tomography of brain, breast and molecular imaging [14]. The real time PAT system has embedded large number of linear array transducers used only for conducting experiment with small animals and this is mainly due to the limited angular view which causes the low resolution and distortion in images. This challenging task resulted in invention of various probe types [15]. A two-dimensional array probe [16] is used in a real-time three-dimensional PAT system and also full angular views for image reconstruction are achieved by ring-shaped probe. The high-speed cross sectional imaging of deep brain of rats *in vivo* is obtained using a full ring array photoacoustic computed tomography (PACT) [17]. The main advantage of this system is that it uses internal illumination with the optical fiber rather than the external illumination which delivers less light to the base of the brain.

PAT is used in the clinical applications such as detection of cancers in breast, prostate and in melanoma cancer screening [8]. There are several image reconstruction algorithms for forming the photoacoustic image and the universal back projection algorithm is adopted for the developed system [9]. Due to the nature of reconstruction and the complexity of the system the photoacoustic image consists of noise in the image, so the target needed to be accurately differentiated between the noises. Among the several image segmentation techniques the active contour models also known as snake [10] is one of the most efficient method used in many applications.

A geometric active contour model algorithm known as Chan-Vese model [11] has been used in this system. Depending on the image constraints, the contour either shrinks or expands over the object to easily segment it from the background. A performance evaluation of the image enhancement algorithm is carried out by obtaining the signal to noise ratio for the results obtained from contour method and other filtering methods. Also, a phantom test is carried out to evaluate the effectiveness of the developed system.

II. Methods and Architecture of Photoacoustic System

A. System Components

The real-time photoacoustic system encapsulates a multi-channel data acquisition board (DAQ) which is designed to collect the measured PA signals from the linear array transducer. A sequential order of execution is performed between signal acquisition and image reconstruction. Fig. 1 shows the complete system design of the developed PAT system which has a PCI extension for an instrumentation (PXI) platform-based DAQ with 50-MHz sampling frequency. It also has 12-bit resolution, 64 analog input channels, and 192 Mb/sec transmission speed. This system utilizes the advantage of direct memory access (DMA) method for image reconstruction and the control program was developed using

Prasannakumar Palaniappan and Dong Ho Shin are with the Advanced Biomedical Imaging Center, Chonbuk National University, Jeonju, South Korea (e-mail: prsna1@ yahoo.co.in, skear@ naver.com).

Chul Gyu Song is with the Electronics Engineering Department, Chonbuk National University, Jeonju, South Korea (phone: +82-63-270-4282; fax: +82-63-270-4282; e-mail: song133436@gmail.com).

Labview software (2010; National Instruments). The source, a Nd:YAG Q-switched laser (NT352-A20-AW; EKSPLA) with a 2-Hz repetition rate was used. A custom-developed trigger controller is dedicated for laser emission and a trigger to generate timing signal.

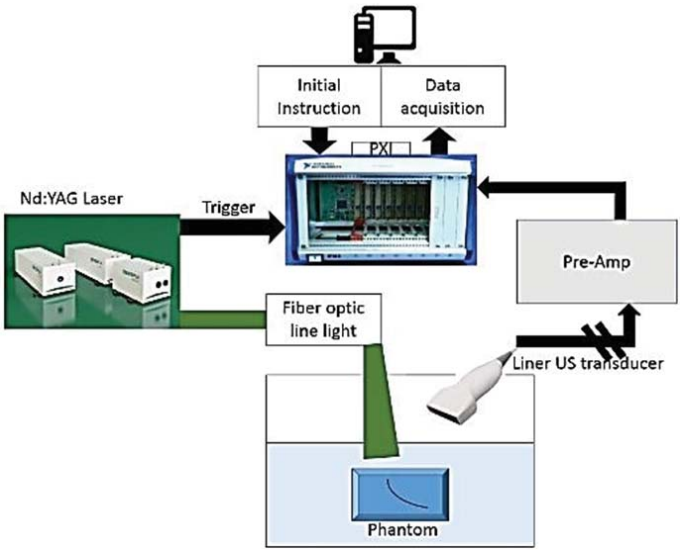

Fig. 1 Hardware block diagram of PAT system

A linear array probe (L14-5/28; Ultrasonix) with a 128 element transducers and 5-MHz center frequency were used to measure the PA signal. A custom-developed pre-amplifier, with 5-MHz passband, 128 channels and 40-dB gain, was placed ahead of the DAQ to amplify and filter the defected signal.

B. Image Reconstruction Algorithm

The construction of the photoacoustic images is performed using the universal back projection algorithm [9]. This algorithm uses the time domain and inverse property of photoacoustic equations. Using (1), the initial source distribution is formed by using the inverse property of the PA equations.

$$P_0 = \int_{\Omega_0} \frac{d\Omega_0}{\Omega_0} \left[2p(\vec{r_0}, v_s t) - 2v_s t \frac{\partial p(\vec{r_0}, v_s t)}{\partial (v_s t)} \right] \quad (1)$$

$$t = \left| \vec{r} - \frac{\vec{r_0}}{v_s} \right| \quad (2)$$

where $\vec{\mathbf{r}}$ is the vector of the final PAI plane and $\vec{\mathbf{r_0}}$ is the sample or measurement point. $\boldsymbol{p(\vec{r_0}, v_s t)}$ is the final photoacoustic signal and the photoacoustic pressure is given by $\mathbf{p_0}$ and the speed of the sound is given by $\mathbf{v_s}$. A constant speed of sound is assumed while obtaining the unified and an exact time domain results. This property uses the limited angular method and enables the use of linear array transducer for signal acquisitions. The number of transducer can be varied depending upon the sample subject and higher the transducer number yields accurate results. The basics of the Fourier domain formulas are used in the reconstruction geometrics to derive the universal back projection algorithm. However, an inhomogeneity in photoacoustics can cause distortion in the image when using the back projection algorithm.

C. Chan-Vese Method and Image Enhancement Algorithm

The most commonly used image segmentation technique is the Otsu global threshold method [12], where a threshold value is defined to separate both the foreground and background. However, in the Chan-Vese method (CVM) the initial object is defined and the contour evolution takes place based on the evolution equation (3). The contour evolution is a process where the initial defined contour either shrink or enlarges. The image plane $P(x,y)$ has an evolving curve E = $\partial\omega$. The energy function is given by:

$$F(e_1, e_2, E)\mu|E| + \lambda_1 \int_{inside(e)} |P(x,y) - e_1|^2 \, dx \, dy + \int_{outside(e)} |P(x,y) - e_2|^2 \, dx \, dy \quad (3)$$

where the outside and inside on E is given by *outside(e)* and *inside(e)*. The constant e_1 and e_2 are the intensities averages of the image. To consider λ_1 and λ_2 to unity, the μ positive constant is used [18]. In order to regularize the contour, $|E|$ is used. Finally, to fix the minimization problem the Euler-Lagrange functions are used in (3) and can be rewritten as:

$$\frac{\partial \phi}{\partial t} = \delta(\phi) \left[\mu div \left(\frac{\nabla \phi}{|\nabla \phi|} \right) - v - \lambda_1 (p - e_1)^2 + \lambda_2 (p - e_2)^2 \right] \quad (4)$$

where ϕ is the energy function defined in relation to the level set method. The initial of the evolving curve can be marked anywhere in the image. The contour can evolve with or without gradients in the image plane and easily segment the desired object.

Once the PAI image is acquired it undergoes the image enhancement algorithm. This algorithm consists of several image processing techniques such as image preprocessing, image binarization, morphological operations and contour filtering as shown in Fig. 2.

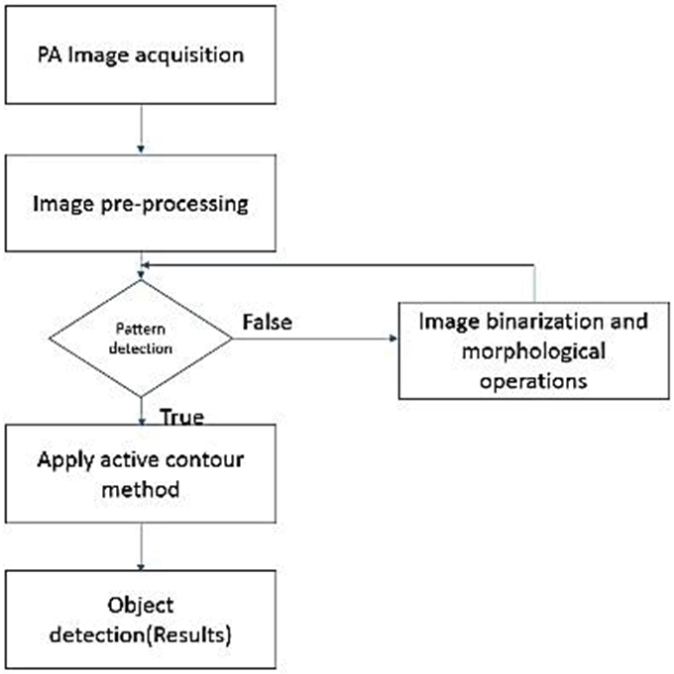

Fig. 2 Image enhancement algorithm using CVM

D.Experiments

To test the ability and reliability of the photoacoustic system a phantom experiment is conducted. The phantom is made upon of water and gelatin in a ratio of 2:8 to imitate a biological specimen. Once the photoacoustic images are acquired, it goes through the image enhancement algorithm. The image enhancement algorithm is developed based on the CVM. Transparent plastic tubes with inner diameter of 300 μm filled with contrast agents such as Indocyanine green (ICG) and Methylene blue. These tubes are placed in between the phantom to imitate the blood vessel in biological tissue. The transparent tubes are placed in a non-uniform length and multiple of these are placed in between the phantom to test the accuracy of the PAT system.

III. Result and Discussion

The PAI images are acquired at different wavelength in a range of 700nm - 900nm to test the ability of the contrast agents. The PAI image with maximum intensity observed were shown in Fig. 3. These images were taken with methylene blue and ICG as agents in transparent tube. This acquired photoacoustic image now goes through the image enhancement algorithm to clearly identify the object. Image preprocessing such as removing of noise using averaging filter is applied and later the algorithm looks for the area of the object. If the tube with desired area as above the threshold value was found, then the CVM is applied or else the image undergoes the morphological opening followed by either dilation or erosion. Once the appropriate area above the threshold is found then the PAI goes through further processing. The results of the tube with contrast agent are shown in Fig. 4 in a pseudo-color image.

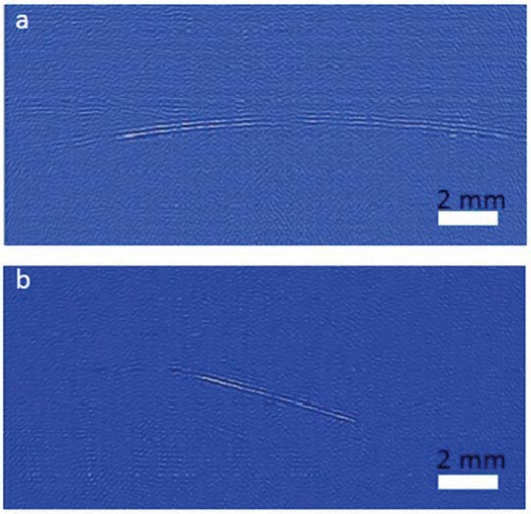

Fig. 3 (a) PAI image with methylene blue as contrast agent at 750nm, (b) PAI image with ICG as contrast agent at 780nm

The efficiency of the contour segmentation is verified by comparing the peak signal to noise ratio (PSNR) and average

root mean square error (ARMSE) of contour segmentation and selective manual segmentation. Even though the selective manual segmentation uses a large amount of time and code complexity, the results are comparable to the contour image enhancement algorithm. The ARMSE and PSNR of both segmentation techniques. It is evident from Table I that active contour filtering was an effective filtering method and it was able to provide acceptable results to accurately delineate the target in PAT. Even though, the active contour filtering is an efficient algorithm; it is also a time burden method. It can be used in a system where time is not a first priority and defining a sample's geometric shape is a main concern.

TABLE I
COMPARISON OF CONTOUR FILTERING AND MANUAL FILTERING

	Manual segmentation	Active contour segmentation
Average root mean square error	6.827	5.273
Signal to noise ratio	27.91 *dB*	29.07 *dB*

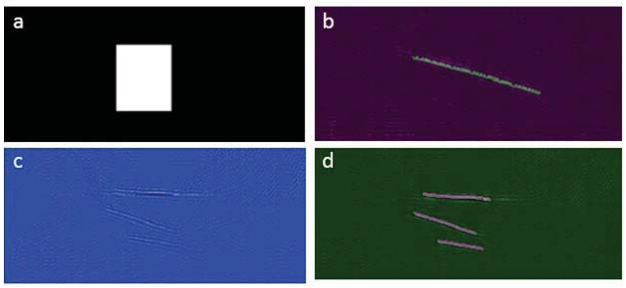

Fig. 4 (a) A 66x55 size of initial mask for contour segmentation, (b) Final contour after 912 iterations using CVM, (c) PAI of ICG in multiple tube, (d) Pseudo-color image of final segmented image using CVM

IV. CONCLUSION

A PAT system is developed and it is capable of reconstructing an image using universal back projection algorithm. The active contour method is used to accurately delineate the target which is imitated using phantom experiment. The optoacoustic images are obtained using methylene blue and indocyanine green at a wavelength of 700-900nm using the developed system. In further studies, a custom developed contour segmentation is developed which can be solely used for photoacoustic image. Even more different segmentation or filtering techniques can be used in image enhancement algorithm. This developed algorithm is proved to be efficient only when processing time is not an important factor. When the PAT system is developed using a graphical processing unit, the time taken by the image enhancement algorithm can be drastically reduced. Also in the next step of developing this study, contrast agents are injected in rats and *in vivo* images are obtained to test the efficiency of both the filter and system.

ACKNOWLEDGMENT

This research work was funded by the Technology Innovation Program (10052749, Development of ultrafast cardiovascular diagnostic system based on the multifunctional 3D ultrasound imaging) funded by the Ministry of Trade, Industry and Energy (MOTIE) of Korea.

REFERENCES

[1] Oraevsky A A, Esenaliev R O, Jacques S L, Tittel S K, "Laser opto-acoustic tomography for medical diagnostics: principles," Proc. SPIE 2976 22.31, 1996.
[2] Wang X, Pang Y, Ku G, Xie X, Stoica G, Wang L V, "Non-invasive laser-induced photoacoustic tomography for structural and functional imaging of the brain in vivo," Nat. Biotechnol. 21 803.6, 2003.
[3] Kruger R A, Liu P-Y, Fang Y, "Thermoacoustic ultrasound (PAUS)-reconstruction tomography," Med. Phys.22 1605.9, 1995.
[4] Lihong V. Wang, "Ed. Photoacoustic Imaging and Spectroscopy," 1st ed., Boca Raton: CRC Press, 2009.
[5] Zhang H F, Maslov K, Stoica G, Wang L-H, "Functional photoacoustic microscopy for high-resolution and noninvasive in vivo imaging," Nat. Biotechnol. 24 848.51, 2006.
[6] A. Oraevsky and A. Karabutov, "Optoacoustic tomography, in Biomedical Photonics Handbook," T. Vo-Dinh, CRC, Boca Raton, Ed., Chap. 34, pp. 1-34, 2003.
[7] L. V. Wang and H. Wu, "Ed. Biomedical Optics: Principles and Imaging," John Wiley, 2007
[8] J. T. Oh, M. L. Li, H. F. Zhang, K. Maslov, G. Stoica, and L. V. Wang, "Three-dimensional imaging of skin melanoma in vivo by dual-wavelength photoacoustic microscopy," J. Biomed. Opt., Vol. 11, No. 3, p. 034032, Nov. 2006.
[9] M Xu, L. V. Wang, "Universal back-projection algorithm for photoacoustic-computed tomography," doi:10.1117/12.589146, 2005.
[10] Kass, Michael, Andrew Witkin, and Demetri Terzopoulos. "Snakes: Active contour models." International journal of computer vision 1.4 (1988): 321-331.
[11] Chan, Tony F., B. Yezrielev Sandberg, and Luminita A. Vese. "Active contours without edges for vector-valued images." Journal of Visual Communication and Image Representation 11.2 (2000): 130-141.
[12] N. Otsu, A threshold selection method from gray-level histograms, IEEE Trans Syst Man Cybern, SMC-0 (1), 62 (1979).
[13] Roger J. Zemp, Liang Song, Rachel Bitton, K. Kirk Shung, and Lihong V. Wang, "Realtime photoacoustic microscopy in vivo with a 30-MHz ultrasound array transducer," doi: 10.1364/OE.16.007915, OSA: 2008
[14] Lihong V. Wang, "Prospects of photoacoustic tomography," The International Journal of Medical Physics Research and Practice, doi: 10.1118/1.3013698, 2008.
[15] R. J. Zemp, R. Bitton, M. L. Li, K. K. Shung, G. Stoica, and L. V. Wang, "Photoacoustic imaging of the microvasculature with a high-frequency ultrasound array transducer," J. Biomed. Opt., Vol. 12 No. 1, p. 010501, Jan./Feb. 2007.
[16] Zhou Q, Ji X, Xing D., "Full-field 3D photoacoustic imaging based on plane transducer array and spatial phase-controlled algorithm," Med. Phys., Vol. 38, No. 3, Mar. 2011.
[17] Li Lin; Jun Xia; Terence T. W. Wong; Lei Li and Lihong V. Wang "In vivo deep brain imaging of rats using oral-cavity illuminated photoacoustic computed tomography", J. Biomed. Opt. 20(1), 016019; Jan 22, 2015.
[18] T. F. Chan, L. A. Vese, Active contours without edges. IEEE Transactions on Image Processing, Volume 10, Issue 2, pp. 266-277, 2001.

Prasannakumar Palaniappan was born in India, on April the 18th, 1988. He received his Bachelor of Engineering in Electronics and Communication at Anna University, India in 2009 and he received Master degree in Electronics Design at Mid-Sweden University, Sweden in 2013. Presently he is a PhD student at Chonbuk National University, South Korea. His research interests are in photoacoustic tomography, machine vision, image processing and development of bio-medical applications.

Doung Ho Shin was born in Korea, on March the 24th, 1986. He received his Bachelor of Engineering in Electronics and Communication at Chonbuk National University, Korea in 2011 and he received Master degree in Electronic engineering at Chonbuk National University, Korea in 2013. Presently he is a PhD student at Chonbuk National University, South Korea.

His research interests are in photoacoustic tomography, Fluorescence Imaging, image processing and development of bio-medical applications.

Chul Gyu Song was born in Korea, on November the 10th, 1962. He received his Bachelor of Electrical Engineering at Yonsei University, Korea in 1988 and he received Master degree in Electrical Engineering at Yonsei University, Korea in 1991 and he received PhD in Bioelectronics at Yonsei University. Presently, he is a professor at Chonbuk National University, South Korea. His research interests are in Bio- medical Engineering, photoacoustic tomography and Optical Coherence Tomography.